Poisson Networked Control Systems: Statistical Analysis and Online Learning for Channel Access

Gourab Ghatak
Dept. of EE
IIT, Delhi, India
gourab.ghatak@ee.iitd.ac.in

Geethu Joseph
Faculty of EECMS
TU Delft, Netherlands
g.joseph@tudelft.nl

Chen Quan
Faculty of EECMS
TU Delft, Netherlands
c.quan@tudelft.nl

***Abstract*—We develop a framework for communication-control co-design in a wireless networked control system with multiple geographically separated controllers and controlled systems. Each controlled system consists of an actuator, plant, and sensor. The locations of the controller-controlled system pairs are modeled using a Poisson point process. Controllers periodically receive system state estimates from their respective sensors and design control inputs accordingly. The inputs are then communicated to the corresponding actuators over a shared wireless channel, leading to interference. Our co-design includes a control strategy at the controller based on sensor measurements and transmission acknowledgments from the actuators, utilizing a block ALOHA protocol for channel access. First, we provide a statistical analysis of the control performance. Then, we introduce a Thompson sampling-based online learning algorithm to optimize channel access via the ALOHA parameter. Finally, our numerical results demonstrate the impact of the choice of the ALOHA parameter on the control performance and the efficacy of the learning algorithm in choosing the optimal ALOHA parameter.**

***Index Terms*—Communication-control co-design, controllability, Poisson point process, shared wireless channel, interference, ALOHA protocol, Thomson sampling, stochastic geometry**

I. Introduction

The rapid evolution of wireless networks and the rising demand for new applications, such as remote surgery in advanced medical systems, robotics in industrial automation, intelligent buildings, and autonomous driving in future transportation systems [1], [2], demand a shift towards real-time control systems based on wireless channels. These networked control systems comprise multiple controllers, sensors, actuators, and plants connected through a shared communication medium. Using shared network resources instead of dedicated resources introduces new design challenges due to the simultaneous design of controller-plant communication protocols and control input design. The critical issues that affect the control performance in a networked control system include unreliable communication links [3], transmission delays [4], time synchronization issues [5], and network access constraints and conflicts [6]. This paper investigates the communication-control design of a large-scale wireless networked control system where the interference from co-channel transmissions of different controllers degrades the control performance.

Prior research has mainly focused on networked control systems with a single controller and plant with one or more actuators and sensors communicating over wireless links. Designing optimal wireless networked control systems requires integrating control and communication theories. Current literature discusses two principal approaches to designing these systems: independent control-communication design [7]–[9] and control-communication co-design [10]–[15]. The independent design approach separates the system into distinct control and communication components, designing each separately. In contrast, the co-design approach integrates communication and control systems, capturing their interactions to enhance overall performance. This integrated approach, which is also our focus, is expected to yield significantly improved system performance compared to independent design methods, making it more suitable for real-time control applications in wireless networks [11].

Furthermore, existing studies have explored several aspects of co-design problems. For example, [10] investigated the use of communication imperfections to stabilize control systems and enhance network security. Further, [16] addressed communication and control co-design under limited communication resources to maintain system reachability and observability when only subsets of sensors and actuators can communicate with the controller at a time. Another model is co-design in cloud-controlled automated guided vehicle systems, assuming lossless sensor-to-controller channels but facing potential packet loss in controller-to-actuator channels [11]. [12] investigated the stability robustness of the overall system in scenarios where state information is missing from sensor to controller. [13] considered an online optimization approach for control and communication co-design where packet losses may occur both from the sensor to the controller and from the controller to the actuator. [14] investigated the joint scheduling and power allocation problem for various sensor-controller pairs or controller-actuator pairs over a shared wireless channel. Gaussian process regression was utilized to predict missing sensor states or actions when access to the shared channel is unavailable. The age-of-information metric was employed to assess the credibility of these predictions. The age-of-information metric was also utilized in [15] to characterize information freshness, aiming to minimize control cost and communication energy consumption.

In short, most co-design methods focus on two types of constrained optimization problems. One type addresses the control system's objective function with communication re-

ISBN 978-3-903176-65-2

quirements as constraints, while the other focuses on designing communication protocols and parameters to achieve specific control performance goals. In control optimization problems, the objective is typically to minimize control costs or optimize control performance metrics (e.g., stabilization and tracking error), while considering constraints like time delay, bandwidth, packet loss probability, number of communication channels and sampling period [17]–[20]. In communication optimization problems, the researchers attempt to optimize the communication performance or minimize the communication cost (e.g., minimize energy consumption, transmission time, or maximizing spectral efficiency), subject to constraints like sampling period, time delay, bandwidth, packet loss probability, and Lyapunov control constraints [18], [21], [22]. While several efforts have been made for joint communication-control designs, large-scale wireless control systems with multiple interfering controllers have not been well-studied in the literature. This paper addresses this issue with a communication-control co-design approach by considering such interfering signals from the randomized locations of control and actuator pairs.

The co-design approach requires an accurate characterization of the interference experienced by the controllers. Stochastic geometry offers an attractive set of tools and techniques to study the impact of different network geometries on the resultant interference. In this work, we employ a homogeneous Poisson point process (PPP) to model the locations of different controllers. The main contributions of this work are as follows.

- *Communication-control co-design:* For the controlled system, we present a communication-control design with a wireless channel acknowledgment-based control input design and a block ALOHA protocol to ensure that the system state is driven to the desired state. Based on the design, we introduce a notion of controllability, called *block controllability*, that depends on the number of consecutive successful transmissions from the controller to the actuator, referred to as the burst length.
- *Statistical analysis:* For the typical controller-controlled system pair in the network, we derive the conditional success probability of a transmission, given a realization of the point process. Additionally, we analyze the conditional distribution $\bar{F}_{B_{\rm RL}}$ of the burst length given a realization of the point process. The meta-distribution of the burst length characterizes the fraction of the controller-controlled system pairs in the network, achieving block controllability. Since deriving the exact meta distribution is challenging, we characterize the system's performance based on the first moment of $\bar{F}_{B_{\rm RL}}$ weighted by the channel access probability.
- *Learning-based channel access:* We present a Thompson Sampling (TS) based algorithm for the sequential selection of the ALOHA parameters in successive blocks in a centralized manner. We demonstrate how our statistical framework effectively supports the TS algorithm. Our study highlights that online learning of the optimal ALOHA parameter can enhance the control performance of the network.

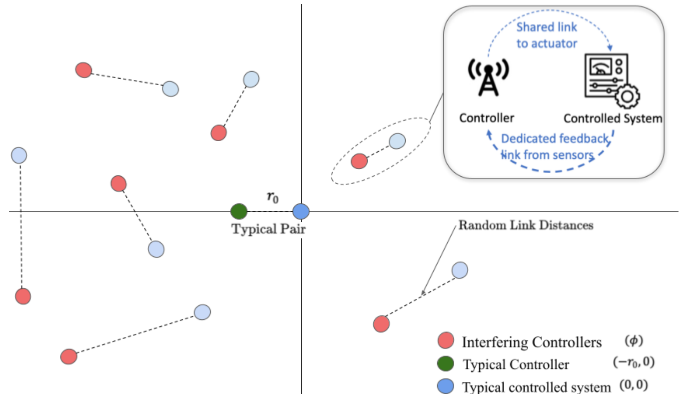

Fig. 1. Illustration of the Poisson network of controller-controlled system pairs. Here, the actuators receive the control input from the corresponding controller via a shared link, whereas the sensors send their observations to the controller via a dedicated link.

Overall, our research establishes new synergies among networked control systems, stochastic geometry, and learning-based channel access strategies, offering valuable insights from both theoretical and algorithmic perspectives.

II. Networked Control System Model

Consider a large network comprising multiple processes and systems, each with its own independent control mechanisms. Each system in the network is represented by a controller-controlled system pair, where the controlled system consists of an actuator, plant, and sensor. We model our network using a Poisson bipolar point process consisting of controller-controlled system pairs in the two-dimensional Euclidean plane $\mathbb{R}^2$ [23]. The locations of the controllers are modeled as a homogeneous PPP Φ of intensity λ. The controller-controlled system pairs are indexed as $i = 0, 1, 2, \ldots$. Without loss of generality, we assume a typical controlled system at the origin, and the typical controller is at a distance of r_0 away from the origin. We note that Slivnyak's theorem [24] guarantees that the process Φ conditioned on the location of the typical pair is a PPP has the same statistics as Φ. The controller-controlled system pair index $i = 0$ refers to the typical pair. Further, r_i denotes the distance between the ith controller and the typical controlled system.

The controller periodically receives the system state from the sensor through a reliable dedicated channel. Based on this system state, it computes the control inputs and communicates them to the actuator via a shared wireless link. Since all controller-actuator pairs utilize the same communication resources (time and frequency), interference can occur, resulting in control performance degradation. Our objective is to design a probabilistic channel access protocol that learns and optimizes the control performance of the system. In the following subsections, we present the various components of our system model.

A. Controller-Controlled System Model

Each controlled system in the network is modeled using a discrete-time linear dynamical system. Specifically, the typical controlled system is given by

$$\boldsymbol{x}(t+1) = \boldsymbol{A}\boldsymbol{x}(t) + \boldsymbol{B}\boldsymbol{u}(t) + \boldsymbol{v}(t). \tag{1}$$

Here, $\boldsymbol{x}(t) \in \mathbb{R}^n$ is the state of the typical controlled system in the network at discrete time t and $\boldsymbol{u}(t) \in \mathbb{R}^m$ and $\boldsymbol{v}(t) \in \mathbb{R}^n$ are its input and process noise, respectively, at time $t \in \mathbb{N}$. Also, $\boldsymbol{A} \in \mathbb{R}^{n\times n}$ and $\boldsymbol{B} \in \mathbb{R}^{n\times m}$ denote the state and input matrices of the system. The system aims to drive and retain the system state at a desired state $\boldsymbol{x}_{\rm des}$ with a suitable choice of control inputs $\boldsymbol{u}(t)$.

We assume the actuator computing capabilities are limited, with all computations being offloaded to the controller. For this, the sensors observe the system state $\boldsymbol{x}(t)$ periodically at time $t = kT$ for $k \in \mathbb{N}$, where the block length T is the delay between two consecutive observations. Here, k is referred to as the block index, and the controller gets the state estimate at the beginning of each block. For simplicity, we assume that the state $\boldsymbol{x}(t)$ is communicated to the controller via a reliable link with dedicated resources, ensuring perfect system state knowledge at the controller at time kT for $k \in \mathbb{N}$.

As the controller receives the state $\boldsymbol{x}(kT)$ at time kT, it estimates the control inputs needed to drive the system to the desired state $\boldsymbol{x}_{\rm des}$. These inputs are sequentially communicated to the actuator via a shared link. The controller transmissions are synchronized with the controlled system evolution in (1). Therefore, the discrete-time index t also denotes the transmission slot index.

Due to noise and interference from the other transmitting controllers, the controlled system may not always correctly decode the received signal, leading to an unsuccessful transmission. The success of the transmission depends on the wireless channel, modeled next.

B. Propagation Characteristics and Transmission Success

Each wireless link experiences fast fading, assumed to be Rayleigh distributed with parameter 1. The fast fading is independent across time and spatially independent across all links. Also, ρ and α denote the path-loss constant and the path-loss exponent of the channel, respectively [25]. We denote the channel noise power as N_0 and the transmit power as P.

The decision of whether a specific controller transmits in a particular time slot t depends on the channel access protocol. Let the channel access state $C_i(t) \in \{0, 1\}$ be the indicator variable representing whether the ith controller transmits at time t, for $i = 0, 1, \ldots$. Here, $i = 0$ refers to the index of the typical controller. Given that the typical controller transmits, the signal to interference plus noise ratio (SINR) at the typical actuator is

$$\xi(t) = \frac{P\rho|h_0(t)|^2 r_0^{-\alpha}}{N_0 + \sum_{i\in\Phi} C_i(t)P\rho|h_i(t)|^2 r_i^{-\alpha}}, \tag{2}$$

where $h_i(t)$ is the channel fading between the ith controller and the typical actuator.

If the SINR at time t exceeds a threshold $\gamma > 0$ (depending on the application and the receiver hardware), the actuator correctly decodes the received signal, thereby implying a successful transmission. The successful transmission by the typical controller at time t is indicated by $S(t) \in \{0, 1\}$, i.e.,

$$S(t) = \begin{cases} 1, & \text{if } C_0(t)\xi(t) > \gamma \\ 0, & \text{otherwise.} \end{cases} \tag{3}$$

Also, the controller receives an acknowledgment of transmission $S(t)$ from the actuator. The controller uses $S(t)$ to design the control inputs and its data transmission, as discussed next.

III. Communication-Control Codesign

The co-design consists of two components: a control input design based on periodic sensor measurements and transmission acknowledgements, and a random access data transmission scheme that operates independently of other sensors and without scheduling by a central unit.

A. Control Input Design

The control input design at the controller is based on its estimate $\hat{\boldsymbol{x}}(t)$ of the system state $\boldsymbol{x}$. Since the noise term $\boldsymbol{v}(t)$ is unknown at the controller, from (1), this estimate is

$$\hat{\boldsymbol{x}}(t) = \boldsymbol{A}^{t-kT}\boldsymbol{x}(kT) + \sum_{\tau=kT}^{t-1} \boldsymbol{A}^{t-\tau-1}S(\tau)\boldsymbol{B}\boldsymbol{u}(\tau), \tag{4}$$

The controller designs v control inputs $\{\boldsymbol{u}(t+\tau), \tau = 0, 1, \ldots, v-1\}$ such that $\boldsymbol{x}_{\rm des} = \hat{\boldsymbol{x}}(t+v)$, i.e.,

$$\boldsymbol{x}_{\rm des} = \boldsymbol{A}^v\hat{\boldsymbol{x}}(t) + \sum_{\tau=0}^{v-1} \boldsymbol{A}^{v-1-\tau}\boldsymbol{B}\boldsymbol{u}(t+\tau). \tag{5}$$

However, we note that for any given states $\boldsymbol{x}_{\rm des}$ and $\hat{\boldsymbol{x}}(t)$, the above equation has a solution if v exceeds the controllability index of the linear dynamical system in (1). Furthermore, the controllability index is further upper-bounded by the degree of the minimum polynomial of $\boldsymbol{A}$ [26]. So, at time $t = kT$, we choose v as the degree of the minimum polynomial of $\boldsymbol{A}$. With this choice, the controller solves (5) using the least squares solution to obtain

$$\begin{aligned} &\begin{bmatrix}\boldsymbol{u}(t)^\mathsf{T} & \boldsymbol{u}(t+1)^\mathsf{T} \ldots \boldsymbol{u}(t+v-1)^\mathsf{T}\end{bmatrix}^\mathsf{T} \\ &\qquad = \boldsymbol{\Psi}^\dagger(v)\left[\boldsymbol{x}_{\rm des} - \boldsymbol{A}^v\hat{\boldsymbol{x}}(t)\right], \end{aligned} \tag{6}$$

with $t = kT$, and for any $L > 0$, we define

$$\boldsymbol{\Psi}(L) = \begin{bmatrix}\boldsymbol{A}^{L-1}\boldsymbol{B} & \boldsymbol{A}^{L-2}\boldsymbol{B} & \ldots & \boldsymbol{B}\end{bmatrix}. \tag{7}$$

If the transmission of $\boldsymbol{u}(kT)$ is successful, i.e., $S(kT) = 1$, it continues to transmit the next control inputs $\boldsymbol{u}(kT+1), \boldsymbol{u}(kT+2), \ldots, \boldsymbol{u}(kT+l)$ until either $S(kT+l) = 0$ or $l = v-1$. If $S(kT+l) = 0$ for some $l < v$, the controller recomputes the next set of v inputs using (6) with $t = kT+l+1$ and repeats the above steps. If $S(kT+l) = 1$ for $l = 0, 1, \ldots, v-1$, all the v control inputs designed by the controller have reached the actuator.

Once all the v control inputs are applied, the state estimate at the controller is $\boldsymbol{x}_{\rm des}$. Then, the next set of inputs required to retain the system state at the desired state $\boldsymbol{x}_{\rm des}$ can be computed as

$$\begin{aligned}\left[\boldsymbol{u}(t)^{\mathsf{T}} \quad \boldsymbol{u}(t+1)^{\mathsf{T}} \ldots \boldsymbol{u}(t+v_{\rm stay}-1)^{\mathsf{T}}\right]^{\mathsf{T}} \\ = \boldsymbol{\Psi}^{\dagger}(v_{\rm stay})\left[\boldsymbol{I}-\boldsymbol{A}^{v}\right]\boldsymbol{x}_{\rm des}, \quad (8)\end{aligned}$$

where $v_{\rm stay}$ is the smallest number of control inputs required to make the system state stay at $\boldsymbol{x}_{\rm des}$ and $\boldsymbol{\Psi}(\cdot)$ is given by (7). However, we note that the above set of $v_{\rm stay}$ control inputs in (8) is independent of the system state and can be computed offline. Consequently, the control inputs given by (8) can be pre-calculated and stored at the actuator. Once the actuator receives v consecutive control inputs from the controller, it can repeatedly use the inputs from (8) without any additional computations till the end of the block where the sensor sends the state information to the controller at time $(k+1)T$.

B. Block ALOHA Protocol and Channel Access Optimization

Under the above Poisson network model, we aim to optimize channel access policy based on actuator acknowledgment $S(t)$ in (3) to maximize its probability of successfully steering its state estimate in (4) to the desired state $\boldsymbol{x}_{\rm des}$. Here, the controller can drive its state estimate to the desired state $\boldsymbol{x}_{\rm des}$ only if v consecutive transmission from the controller to the actuator is successful. This notation of control performance is captured by the random event defined below.

Definition 1. *Consider the typical system $(\boldsymbol{A}, \boldsymbol{B})$ with v being the degree of the minimum polynomial of $\boldsymbol{A}$. The system is said to* block controllable *in a given block k if there is a run of at least v ones in the sequence $S(kT), S(kT+1), \ldots, S((k+1)T-1)$, where $S(t) \in \{0,1\}$ given by* (3) *denotes the success of transmission from the typical controller to the typical actuator at time t.*

We use a modified version of the ALOHA protocol, called *block ALOHA*, for the controller channel access. In block ALOHA channel access protocol, each controller is either active or idle during an entire block k with a probability $q \in \mathcal{P}$ selected from a finite set of D access probabilities $\mathcal{P} \coloneqq \{p_1, p_2, \ldots, p_D\}$ [27]. The channel access probability q is called the block ALOHA parameter. Therefore, the channel access state $C_i(t)$ for $i = 0, 1, \ldots$ is the same for all values of $t = kT, kT+1, \ldots, (k+1)T-1$ within a given block k.

Under this protocol, controllers continues to transmit even after v successful transmissions. Following these v transmissions, the controller sends dummy data to the actuator. The actuator then uses the pre-calculated control input as specified by (8) instead of the transmitted signals. Nonetheless, the actuator continues to send acknowledgments $S(t)$ upon successfully receiving data from the controller. This feedback helps the controller learn its channel conditions and adjust the block ALOHA parameter accordingly. In short, in every block k, the controller decides to transmit with probability q. If the controller decides to transmit, it follows that above control design and data transmission, summarized in Algorithm 1.

Algorithm 1 Control Design and Data Transmission of Typical Controller

Parameters: Block k, system matrices $\boldsymbol{A}, \boldsymbol{B}$, desired state $\boldsymbol{x}_{\rm des}$
Initialization: Time $t = kT$, Burst length $L = 0$
Define $v =$ the degree of the minimum polynomial of $\boldsymbol{A}$
Receive $\hat{\boldsymbol{x}}(kT) = \boldsymbol{x}(kT)$ from the sensor
for $t = kT, kT+1, \ldots, (k+1)T-1$ **do**
// if the last tx fails, redesign inputs
  if $L = 0$ **then**
    Compute $\boldsymbol{u}(t), \boldsymbol{u}(t+1), \ldots, \boldsymbol{u}(t+v-1)$ via (6)
// if block controllable, transmit dummy data
  else if $L = v$ **then**
    Set $\boldsymbol{u}(t) = \mathbf{1}$
  end if
  Transmit $\boldsymbol{u}(t)$ and receive $S(t)$
// if the tx fails, set burst length =0
  if $S(t) = 0$ **then**
    Set $L = 0$
// if the tx succeeds, update burst length
  else
    Update $L \leftarrow \max\{L+1, v\}$
  end if
end for

Next, we aim to optimally choose block ALOHA parameter $q \in \mathcal{P}$ of the typical controller to maximize the number of blocks in which the typical control system is block controllable. Here, the typical controller is unaware of the spatial configuration (density and locations) of the interfering controller-controlled system pairs in the network, as well as their transmission states. However, the controller receives acknowledgment $S(t)$ from the actuator, which it uses to adapt its channel access strategy. In the following section, we discuss the statistical analysis of control performance via block controllability.

IV. Statistical Analysis of Control Performance

From Definition 1, block controllability requires at least v consecutive successful transmission in block k. We refer to the length of a run of consecutive successful transmission as the burst length L of at least v. To optimize the block ALOHA parameter q, we define and characterize the spatiotemporal statistics of the burst length. We begin by deriving the probability of a successful transmission at a given time t when the typical pair transmits.

Proposition 1. *Consider a network following a given PPP Φ, whose ith controller is at a distance of r_i from the typical actuator, and C_i indicates whether or not it transmits in a given block k of T slots. Given that the typical controller transmits in block k, the conditional success probability $P_{\rm s}$*

of the typical controller at a given time t within the block is given by

$$P_{\mathrm{s}} = e^{-\frac{\gamma N_0}{P\rho r_0^{-\alpha}}} \prod_{i\in\Phi:\, C_i=1} \frac{r_0^{-\alpha}}{r_0^{-\alpha}+\gamma r_i^{-\alpha}}, \tag{9}$$

where the parameters P, ρ, N_0 and α are defined in (2) *and γ is the SINR threshold for successful transmission in* (3)*.*

Proof: See Appendix A. ■

We note that conditioned on Φ, the above success event is independent across the time slots when the typical controller transmits. Also, the probability P_{s} changes across blocks as C_i changes. The next important aspect is to characterize the burst length L and compute the probability that it exceeds the desired length v.

Remark 1. *Leveraging de Moivre's solution [28, Section 22.6], for a given block k, the conditional complementary cumulative distribution function (CCDF) $\bar{F}_{B_{\mathrm{RL}}}(\nu) = \mathbb{P}(L \geq \nu \mid \Phi)$ of burst length L as a function of P_{s} is*

$$\bar{F}_{B_{\mathrm{RL}}}(\nu) = \sum_{l=1}^{\lfloor\frac{T+1}{\nu+1}\rfloor} (-1)^{l+1}\left(P_{\mathrm{s}} + \frac{T-l\nu+1}{l}(1-P_{\mathrm{s}})\right) \times \binom{T-l\nu}{l-1} P_{\mathrm{s}}^{l\nu}(1-P_{\mathrm{s}})^{l-1}. \tag{10}$$

With $\nu = v$ in (10), we derive the probability of block controllability as given below.

Proposition 2. *Consider a network following a given PPP Φ described in Proposition 1. Given that the typical controller transmits in block k, the probability that the system is block controllable is $\bar{F}_{B_{\mathrm{RL}}}(v)$, where $\bar{F}_{B_{\mathrm{RL}}}(\cdot)$ is defined in* (10)*.*

The above result establishes the probability of block controllability for a given realization of PPP ϕ with a given value of C_i for the controllers. Next, we look at the control performance averaged over the network realization using the moments of conditional success probability.

Theorem 1. *Consider a network following a given PPP Φ with density λ and block ALOHA parameter q. Given that the typical controller transmits, the probability P_{blk} of block controllability for the typical pair is*

$$P_{\mathrm{blk}} = \mathbb{E}\left[\bar{F}_{B_{\mathrm{RL}}}(v)\right] = \sum_{l=1}^{\lfloor\frac{T+1}{v+1}\rfloor} (-1)^{l+1}\binom{T-lv}{l-1} \times \left(\sum_{\ell=0}^{l-1}\binom{l-1}{\ell}(-1)^{\ell}\zeta(lv+1+\ell) + \frac{T-lv+1}{l}\sum_{\ell=0}^{l}\binom{l}{\ell}(-1)^{\ell}\zeta(lv+\ell)\right). \tag{11}$$

Here, with the parameters P, ρ, N_0 and α in (2)*, γ is the SINR threshold for successful transmission in* (3)*, we define*

$$\zeta(l) = e^{-\frac{\gamma N_0 l}{P\rho r_0^{-\alpha}}} \exp\left(2\pi\lambda q I_l\right), \tag{12}$$

with the function I_l given as

$$I_l = \sum_{\ell=1}^{l}\binom{l}{\ell}\int_0^{\infty}\left(\frac{-\gamma z^{-\alpha}}{r_0^{-\alpha}+\gamma z^{-\alpha}}\right)^{\ell} \mathrm{d}z. \tag{13}$$

Proof: See Appendix B. ■

Further, we can define the meta-distribution of the burst length L as the distribution of $\bar{F}_{B_{\mathrm{RL}}}(v)$, i.e.,

$$\mathcal{M}_B(v,\beta) = \mathbb{P}\left(\bar{F}_{B_{\mathrm{RL}}}(v) \geq \beta\right),$$

where $\bar{F}_{B_{\mathrm{RL}}}(v) = \mathbb{P}(L \geq v \mid \Phi)$ is the conditional CCDF of L as defined in (10). In other words, $\mathcal{M}(v,\beta)$ represents the fraction of control systems in the network that experience a burst length of at least v in a sequence of T transmissions in at least β fraction of the network realization (or equivalently, due to ergodicity, in at least β fraction of transmissions episodes). Unlike the meta-distribution of the SINR in wireless networks, we observe that the meta-distribution of the burst length is challenging to derive even indirectly via its moments. However, if all the controllers have the same desired burst length v, the first moment of the distribution is given by $\mathbb{E}\left[\bar{F}_{B_{\mathrm{RL}}}(v)\right]$ in Theorem 1.

To summarize, this section studied the statistical properties of the block controllability of our networked control system. The analysis focused on the probability of block controllability, assuming that the typical controller transmits in the block of interest. Also, the probability of block controllability without conditioning on the transmission of typical control is given by qP_{blk}, accounting for the block ALOHA parameter's impact on the controlled system's performance.

Moreover, for a given network realization, the optimum value of the block ALOHA parameter depends on the locations of the controllers. It is impractical to have global knowledge of the concurrent active devices in the network at each controller. Therefore, the controllers can only learn the optimum value of the block ALOHA parameter through the acknowledgments sent by the actuators. In the next section, we discuss a TS-based learning algorithm to optimize the block ALOHA parameter selection.

V. Thompson Sampling-Based Block ALOHA Parameter Selection

In this section, we present a simple centralized optimal channel access learning policy based on the derived framework in the previous section. This reinforces the efficacy of statistical analysis in developing such online algorithms.

We consider that a central decision-maker that broadcasts the block parameter $q(k) \in \mathcal{P}$ to all the controllers in the network at the beginning of the block k. Then, the individual controllers set their channel access states C_i probabilistically based on this parameter. The central decision-maker receives the T acknowledgments for each transmitting (active) controller and uses them to update the channel access probability. The goal of the decision-maker is to sequentially select channel access probabilities $q(1), q(2), \ldots, q(K)$ to maximize the probability of block controllability of the typical pair.

A. Multiarm Bandit Formulation

We formulate the decision-maker's task of sequentially selecting channel access probabilities across blocks as a multi-armed bandit (MAB) problem. Here, the set of D access probabilities $\mathcal{P} := \{p_1, p_2, \dots, p_D\}$ represents the arms or actions. We observe the corresponding block controllability for every choice of arm, and the probability of block controllability can be learned over different blocks.

To complete the MAB formulation, we also need to define the notion of reward, which should capture the block controllability. One naive approach for reward design is to assign reward one if the typical pair is block controllable and zero otherwise. However, we know that the block controllability increases with P_{s} in Proposition 1. Also, given ϕ and $q(k)$, the rewards are independent and identically distributed across the slots. Therefore, the reward can be formulated based on the number of successful transmissions within a block. Consequently, an alternative reward formulation can set the reward to one if the transmission is successful, i.e., $S(t) = 1$ and zero otherwise. This formulation rewards the channel access probabilities that result in a higher likelihood that the typical controller will experience a successful burst in the subsequent blocks. Since we have more rewards per block, this reward design leads to faster learning than the naive scheme.

We aim to maximize the sum of collected rewards, maximizing the "controllable" blocks. Over a horizon of K blocks, the control performance in terms of the regret is defined as the evolution of the number of selections of the sub-optimal block ALOHA parameter. In contrast to the typical bandit frameworks, we have an additional layer of assessment, wherein the expected value of the regret is obtained not only by averaging over the sample paths of the policy χ, but also over the network realizations Φ. Mathematically,

$$\mathcal{R}(K) = \mathbb{E}_{\chi,\Phi}\left[\sum_{k=1}^{K} \mathbb{1}\left(q(k) \neq q^*\right)\right],$$

where q^* is the optimum block ALOHA parameter. For this, we study a Bayesian approach for the MAB problem, based on TS, as presented next.

B. TS-based Learning

In the TS framework, the decision-maker chooses the block ALOHA parameter based on its belief for the expected reward with each access probability in $\mathcal{P}$. Specifically, the decision-maker starts with a prior probability θ_j of obtaining a reward of one when the block ALOHA parameter $p_j \in \mathcal{P}$ is chosen, and a reward of zero with probability $1-\theta_j$ [29]. Each θ_k is an action's success probability or mean reward. In the Bayesian model, θ_j is modeled as a Beta distribution (conjugate prior for the Bernoulli rewards) with parameters a_j and b_j. For a selected block ALOHA parameter $q(k) = p_j$ in a block k, if the typical controller is active, it experiences a reward of $S(t)$ for a given t in the block k. Based on this reward, the posterior distribution of the chosen access probability p_j is updated using the Bayes'rule [29]. The Bernoulli rewards facilitate a simple update rule: the parameter a_j is incremented by 1 if $S(t) = 1$, while the parameter b_j is decreased by one if $S(t) = 0$. Nonetheless, the block ALOHA parameter does not change until the next block begins. Therefore, we can do a batch update of the parameters at the end of a block. Particularly, at the end of block k, the parameter a_j is incremented by $\sum_{t=kT}^{(k+1)T-1} S(t)$, while the parameter b_j is incremented by $T - \sum_{t=kT}^{(k+1)T-1} S(t)$. Since the typical pair is randomly selected from the distribution of the pairs in the network, the central transmitter can either randomize the pair's selection for observation or consider the average successes across all the pairs in the network. The overall algorithm is summarized in Algorithm 2.

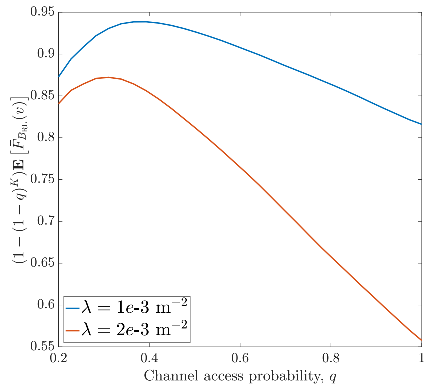

Fig. 2. First moment (mean) of the conditional CCDF of the burst length weighted by the probability that the controller accesses the channel in at least one block. Please refer to Theorem 1 for details.

Algorithm 2 TS for Block ALOHA Parameter Selection

Parameters: Beta distribution parameters $\{(a_j, b_j\}_{j=1}^{D}$
Initialization: $a_j = b_j = 1, \forall j \in \{1, 2, \dots D\}$
for $k = 0, 1, 2, \dots, K$ **do**
  Sample $\theta_j \sim \mathcal{B}(a_j, b_j) \forall j \in \{1, 2, \dots D\}$
  Select probability $q(k) = p_J$, where $J = \arg\max_j \theta_j$
  Observe acknowledgments $S(kT+\tau)$ for $\tau = 0, 1, \dots, T-1$
  Update $a_J \leftarrow a_J + \sum_{\tau=0}^{T-1} S(kT+\tau)$
  Update $b_J \leftarrow b_J + T - \sum_{\tau=0}^{T-1} S(kT+\tau)$.
end for

VI. Numerical Results and Discussion

In this section, we present some numerical results to highlight the salient features of our analysis. Unless otherwise stated, we assume a transmit power of $P = 24$ dBm, a path-loss exponent of $\alpha = 2$ considering line-of-sight propagation. The carrier frequency is assumed to be 3.2 GHz with an operating bandwidth of 200 MHz. The distance between the typical controller-controlled system pair is set as 10 m.

The impact of the block ALOHA parameter on the probability of block controllability is studied in Fig. 2. Here, we plot the expected value of the conditional CCDF of the burst length multiplied by the probability that the typical controller

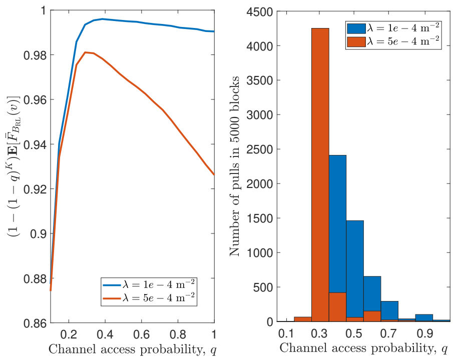

Fig. 3. Comparison of the joint probability of channel access and successful burst of length $v = 5$ in a block length of $T = 20$ and the relative selection of the candidate channel access probabilities by the TS framework in 5000 blocks.

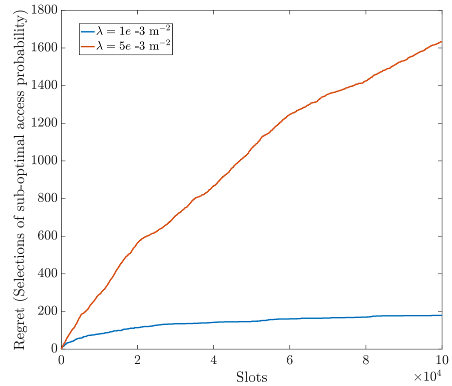

Fig. 4. Expected regret expressed in the number of selections of the sub-optimal access probability as a function of the slot index.

is allowed to transmit in at least one block. For lower values of channel access probabilities, the typical controller has a lower probability of channel access, and hence the effective value of weighted $P_{\text{blk}} = \mathbb{E}\left[\bar{F}_{B_{\text{RL}}}(v)\right]$ is low, even though the transmissions experience lower interference. As the value of q increases, the effective weighted $P_{\text{blk}} = \mathbb{E}\left[\bar{F}_{B_{\text{RL}}}(v)\right]$ increases since the controller accesses the channel with a higher probability. However, further increasing q deteriorates the performance after a threshold of access probability. Indeed, for a high q, although the typical controller accesses the channel more frequently, each time it transmits, it experiences a higher interference from the system, leading to a degradation of the success probability and the likelihood that it experiences a successful burst.

In our centralized TS-based learning of optimal access probability, the access probability for a block is determined based on the sequence of action-reward pairs for the previous blocks. In Fig. 3, we show the variation of the effective success probability (i.e., the weighted $P_{\text{blk}} = \mathbb{E}\left[\bar{F}_{B_{\text{RL}}}(v)\right]$) for one such scenario. We consider the action set to be a discrete one consisting of $D = 10$ probabilities (arms) $\{0.1, 0.2, \ldots, 1\}$. From the statistical framework, note that the optimal block ALOHA parameter for this case is 0.3. We observe that the TS algorithm efficiently learns this parameter relatively quickly. In particular, in 5000 blocks, the system selects the optimum block ALOHA parameter in more than 4500 blocks.

Finally, we show the evolution of the regret, defined as the number of selections (pulls) of the sub-optimal ALOHA parameters for 10^5 blocks in Fig. 4. For lower densities, we observe that the system suffers a lower regret than higher densities. A higher intensity of interfering controllers may degrade the learning performance. Nonetheless, we note that the regret in either case evolves sub-linearly, demonstrating the algorithm's efficacy.

VII. Conclusion

We presented a control design and communication protocol for Poisson networked control systems. Using stochastic geometry, we analyzed interference impacts on network control performance, finding that dense networks with simultaneous channel access by all controllers degrade performance. To mitigate this, we introduced a block ALOHA protocol for the channel access. We studied how the ALOHA parameter influences the probability of successful control input bursts and identified an optimal block ALOHA parameter based on system parameters, such as controller density. Further, we developed a TS algorithm to sequentially optimize this parameter, showing sub-linear regret in finding the optimal parameter. Future work includes theoretically characterizing regret of TS across different network realizations, and analyzing decentralized ALOHA parameter selection.

Appendix A
Proof of Proposition 1

Given the distances r_i's and using (2), the success probability $P_{\text{s}} = \mathbb{P}(\xi(t) > \gamma)$ is given by

$$P_{\text{s}} = \mathbb{P}\left(|h_0(t)|^2 > \frac{\gamma[N_0 + \sum_{i\in\Phi} P\rho|h_i(t)|^2 r_i^{-\alpha} C_i]}{P\rho r_0^{-\alpha}}\right)$$
$$\stackrel{(a)}{=} e^{-\frac{\gamma N_0}{P\rho r_0^{-\alpha}}} \mathbb{E}\left[\exp\left(\frac{-\gamma \sum_{i\in\Phi} \rho r_i^{-\alpha}}{r_0^{-\alpha}} |h_i(t)|^2 C_i\right)\right]$$
$$\stackrel{(b)}{=} e^{-\frac{\gamma N_0}{P\rho r_0^{-\alpha}}} \prod_{i\in\Phi} \mathbb{E}\left[\exp\left(\frac{-\gamma r_i^{-\alpha}}{r_0^{-\alpha}} |h_i(t)|^2 C_i(t)\right)\right],$$

where Step (a) is because $|h_0(t)|^2$ is exponential distributed. Step (b) follows as $h_i(t)$'s are independent across different values of i. Finally, the desired result follows from the Laplace transform of the exponentially distributed $|h_i(t)|^2$. ■

Appendix B
Proof of Theorem 1

From (10), the expected value of $\bar{F}_{B_{\text{RL}}}(v)$ is given by

$$\mathbb{E}\left[\bar{F}_{B_{\text{RL}}}(v)\right] = \sum_{l=1}^{\lfloor \frac{T+1}{v+1} \rfloor} (-1)^{l+1} \binom{T - lv}{l-1}$$
$$\times \mathbb{E}\left[P_{\text{s}}^{lv+1}(1 - P_{\text{s}})^{l-1} + \frac{T - lv + 1}{l} P_{\text{s}}^{lv}(1 - P_{\text{s}})^{l}\right].$$

Using the Binomial expansion $(1-P_{\rm s})^l = \sum_{\ell=0}^{l}\binom{l}{\ell}(-1)^\ell P_{\rm s}^\ell$, we arrive at

$$\begin{aligned}\mathbb{E}\left[\bar{F}_{B_{\rm RL}}(v)\right] = & \sum_{l=1}^{\lfloor \frac{T+1}{v+1} \rfloor} (-1)^{l+1}\binom{T-lv}{l-1} \\ & \times \left(\sum_{\ell=0}^{l-1}\binom{l-1}{\ell}(-1)^\ell \mathbb{E}\left[P_{\rm s}^{lv+1+\ell}\right] \right. \\ & \left. + \frac{T-lv+1}{l}\sum_{\ell=0}^{l}\binom{l}{\ell}(-1)^\ell \mathbb{E}\left[P_{\rm s}^{lv+\ell}\right] \right). \quad (14)\end{aligned}$$

Finally, using the moments of the conditional success probability as follows:

$$\mathbb{E}\left[P_{\rm s}^l\right] = e^{-\frac{l\gamma N_0}{P\rho r_0^{-\alpha}}}\mathbb{E}\left[\prod_{i\in\Phi}\left(\frac{r_0^{-\alpha}}{r_0^{-\alpha}+\gamma r_i^{-\alpha}}\right)^l\right].$$

Here, we note that transmitting controllers follow a homogeneous PPP of intensity λq. So, using the probability generating functional of the PPP [30], we obtain

$$\begin{aligned}&\mathbb{E}\left[\left(\prod_{i\in\Phi}\frac{r_0^{-\alpha}}{r_0^{-\alpha}+\gamma r_i^{-\alpha}}\right)^l\right] \\ &= \exp\left(-2\pi\lambda q\int_0^\infty 1-\left(\frac{r_0^{-\alpha}}{r_0^{-\alpha}+\gamma z^{-\alpha}}\right)^l {\rm d}z\right) \\ &= \exp\left(-2\pi\lambda q\int_0^\infty 1-\left(1-\frac{\gamma z^{-\alpha}}{r_0^{-\alpha}+\gamma z^{-\alpha}}\right)^l {\rm d}z\right).\end{aligned}$$

Further, from the binomial expansion

$$(1-y)^l - 1 = \sum_{\ell=1}^{l}\binom{l}{\ell}(-y)^\ell, \quad (15)$$

with $y = \frac{\gamma z^{-\alpha}}{r_0^{-\alpha}+\gamma z^{-\alpha}}$, we get $\zeta(l) = \mathbb{E}\left[P_{\rm s}^l\right]$. The desired result is obtained by substituting this relation in (14). ■

References

[1] L. Ding, Q.-L. Han, E. Sindi *et al.*, "Distributed cooperative optimal control of DC microgrids with communication delays," *IEEE Trans. Ind. Inform.*, vol. 14, no. 9, pp. 3924–3935, 2018.

[2] Z. Lu and G. Guo, "Control and communication scheduling co-design for networked control systems: A survey," *Int. J. Syst. Sci.*, vol. 54, no. 1, pp. 189–203, 2023.

[3] J. Hu, Z. Wang, G.-P. Liu, H. Zhang, and R. Navaratne, "A prediction-based approach to distributed filtering with missing measurements and communication delays through sensor networks," *IEEE Trans. Syst. Man Cybern.: Syst.*, vol. 51, no. 11, pp. 7063–7074, 2020.

[4] B. Ning, Q.-L. Han, and L. Ding, "Distributed finite-time secondary frequency and voltage control for islanded microgrids with communication delays and switching topologies," *IEEE Trans. Cybern.*, vol. 51, no. 8, pp. 3988–3999, 2020.

[5] D. Baumann, F. Mager, M. Zimmerling, and S. Trimpe, "Control-guided communication: Efficient resource arbitration and allocation in multi-hop wireless control systems," *IEEE Control Syst. Lett.*, vol. 4, no. 1, pp. 127–132, 2019.

[6] K. Gatsis, M. Pajic, A. Ribeiro, and G. J. Pappas, "Opportunistic control over shared wireless channels," *IEEE Trans. Autom. Control*, vol. 60, no. 12, pp. 3140–3155, 2015.

[7] V. Kawadia and P. R. Kumar, "A cautionary perspective on cross-layer design," *IEEE Wirel. Commun.*, vol. 12, no. 1, pp. 3–11, 2005.

[8] M. S. Mahmoud, *Control and estimation methods over communication networks*. Springer, 2014.

[9] J. P. Hespanha, P. Naghshtabrizi, and Y. Xu, "A survey of recent results in networked control systems," *Proc. IEEE*, vol. 95, no. 1, pp. 138–162, 2007.

[10] D. Zhang, Q.-L. Han, and X. Jia, "Network-based output tracking control for a class of TS fuzzy systems that can not be stabilized by nondelayed output feedback controllers," *IEEE Trans. Cybern.*, vol. 45, no. 8, pp. 1511–1524, 2014.

[11] Y. Qiao, Y. Fu, and M. Yuan, "Communication-control co-design in wireless networks: A cloud control AGV example," *IEEE Internet Things J.*, vol. 10, no. 3, pp. 2346–2359, 2022.

[12] S. Hu and W.-Y. Yan, "Stability robustness of networked control systems with respect to packet loss," *Automatica*, vol. 43, no. 7, pp. 1243–1248, 2007.

[13] X. Cao, P. Cheng, J. Chen, and Y. Sun, "An online optimization approach for control and communication codesign in networked cyber-physical systems," *IEEE Trans. Ind. Inform.*, vol. 9, no. 1, pp. 439–450, 2012.

[14] A. M. Girgis, J. Park, M. Bennis, and M. Debbah, "Predictive control and communication co-design via two-way Gaussian process regression and AoI-aware scheduling," *IEEE Trans. Commun.*, vol. 69, no. 10, pp. 7077–7093, 2021.

[15] X. Wang, C. Chen, J. He, S. Zhu, and X. Guan, "AoI-aware control and communication co-design for industrial IoT systems," *IEEE Internet Things J.*, vol. 8, no. 10, pp. 8464–8473, 2020.

[16] L. Zhang and D. Hristu-Varsakelis, "Communication and control co-design for networked control systems," *Automatica*, vol. 42, no. 6, pp. 953–958, 2006.

[17] B. Chang, G. Zhao, Z. Chen, L. Li, and M. A. Imran, "Packet-drop design in URLLC for real-time wireless control systems," *IEEE Access*, vol. 7, pp. 183 081–183 090, 2019.

[18] M. Eisen, M. M. Rashid, K. Gatsis, D. Cavalcanti, N. Himayat, and A. Ribeiro, "Control aware radio resource allocation in low latency wireless control systems," *IEEE Internet Things J.*, vol. 6, no. 5, pp. 7878–7890, 2019.

[19] K. Gatsis, A. Ribeiro, and G. J. Pappas, "State-based communication design for wireless control systems," in *Proc. IEEE Conf. Decision Control*, 2016, pp. 129–134.

[20] L. Scheuvens, T. Hößler, A. N. Barreto, and G. P. Fettweis, "Wireless control communications co-design via application-adaptive resource management," in *Proc. IEEE 5G World Forum*, 2019, pp. 298–303.

[21] P. Park, J. Araújo, and K. H. Johansson, "Wireless networked control system co-design," in *Proc. Int. Conf. Netw. Sens. Control*, 2011, pp. 486–491.

[22] B. Chang, L. Zhang, L. Li, G. Zhao, and Z. Chen, "Optimizing resource allocation in URLLC for real-time wireless control systems," *IEEE Trans. Veh. Technol.*, vol. 68, no. 9, pp. 8916–8927, 2019.

[23] M. Haenggi, "The meta distribution of the SIR in Poisson bipolar and cellular networks," *IEEE Trans. Wirel. Commun*, vol. 15, no. 4, pp. 2577–2589, 2015.

[24] S. N. Chiu, D. Stoyan, W. S. Kendall, and J. Mecke, *Stochastic geometry and its applications*. John Wiley & Sons, 2013.

[25] 3GPP, "Technical specification group radio access network; study on channel model for frequencies from 0.5 to 100 GHz (release 16), document TR," *38.901, version 16.0.0.*, Oct. 2019.

[26] C.-T. Chen, *Linear system theory and design*. Saunders College publishing, 1984.

[27] F. Baccelli, B. Blaszczyszyn, and P. Muhlethaler, "An aloha protocol for multihop mobile wireless networks," *IEEE Trans. Inf. Theory*, vol. 52, no. 2, pp. 421–436, 2006.

[28] A. Hald, *A history of probability and statistics and their applications before 1750*. John Wiley & Sons, 2005.

[29] D. J. Russo, B. Van Roy, A. Kazerouni, I. Osband, Z. Wen *et al.*, "A tutorial on thompson sampling," *Found. Trends Mach. Learn.*, vol. 11, no. 1, pp. 1–96, 2018.

[30] M. Haenggi, *Stochastic geometry for wireless networks*. Cambridge University Press, 2012.